Acta Polytechnica **60**(3):259–267, 2020
DOI:10.14311/AP.2020.60.0259

NEURINGER-ROSEINWEIG MODEL BASED LONGITUDINALLY ROUGH POROUS CIRCULAR STEPPED PLATES IN THE EXISTENCE OF COUPLE STRESS

Yogini Devendrasinh Vashi[a,*], Rakesh Manilal Patel[b], Gunamani Biswanath Deheri[c]

[a] *Gujarat Technological University, Alpha College of Engineering and Technology, Kalol, 382721 Gujarat, India*
[b] *Gujrat University, Gujarat Arts and Science College, Ahmedabad, 380006 Gujarat, India*
[c] *Sardar Patel University, Department of Mathematics Vallabh vidyanagar, 388120 Gujarat, India*
[*] corresponding author: yogini.vashi@gmail.com

Abstract. This study intents to scrutinize the impact of ferrofluid in the presence of couple stress for longitudinally rough porous circular stepped plates. The influence of longitudinal surface roughness is developed using the stochastic model of Christensen and Tonder for nonzero mean, variance and skewness. Neuringer-Roseinweig model is adopted for the influence of ferrofluid. The couple stress effect is characterized by Stoke's micro continuum theory. The modified Reynolds' type equation is stochastically averaged and solved by no-slip boundary conditions. The closed form solutions for load bearing capacity and film pressure are obtained as a function of different parameters and plotted graphically. It is perceived that the load capacity gets elevated owing to the combined influence of magnetization and couple stress when the proper choice of roughness parameters (negatively skewed, standard deviation) is in place. Porosity and roughness (positively skewed) adversely affect bearing's performance. The graphical and tabular analysis shows that there is a significant growth in load bearing capacity compared to the conventional lubricant case.

Keywords: Load bearing capacity, ferrofluid, longitudinal roughness, circular stepped plates.

1. Introduction

A ferrofluid is a liquid that contains a colloidal suspension of ferromagnetic particles and that becomes strongly magnetized in the existence of an external magnetic field. The use of ferrofluid as a lubricant can be found in bearings, loudspeakers, dampers, sensor as well as in biomedical instruments. Several investigators have also attempted to discover its use as a lubricant in squeeze film bearing structures. Bhat and Deheri [1] studied squeeze film characteristic in the curved circular disk by considering the magnetic effect and found that bearing's load capacity is enhanced due to the magnetization parameter. Shah [2] analysed the impact of ferrofluid lubrication in step bearing. Kumar et. al. [3] considered the influence of ferrofluid on spherical and conical bearings using perturbation analysis. Shah and Bhat studied [4] the impact of magnetic fluid on curved annular plates. They considered the revolution of magnetic particles and its magnetic moments. Their study revealed that the load capacity and response time of the bearing improved due to Langevin's parameter. Agrawal [5] examined the impact of porous inclined slider bearing with magnetic fluid and deduced that bearing's life span is longer compared to the viscous porous inclined slider bearing.

Additives have been added in the fluid to create the flow properties and to enhance the lubricating qualities. Couple stress and micropolar fluids are examples of such types of fluids, which have become more important for current industrial materials. Extensive studies have been carried out to describe the importance of the couple stress fluid in different bearing geometries. Ramanaiah and Sarkar [6] analysed the upshot of couple stress for the thrust bearing. Lin [7] made a theoretical study of a squeeze film based finite journal bearing with a couple stress fluid and concluded that squeeze film-based finite journal bearing's characteristics is enhanced due to rheological properties of the couple stress fluid. Maiti [8] analysed the performance characteristic of the composite and step slider bearing with micropolar fluid. He has derived the expression of the load supporting capacity and skin friction using numerical computation and found that the micropolar fluid offers better load supporting capacity compared to a Newtonian fluid. Lin et al. [9] studied the combined performance of couple stress and convective inertia on wide parallel plates and concluded that there is an improvement in the load-carrying capacity and in the response time due to a combined effect of couple stress and convective inertia. Naduvinamani and Siddangouda [10] considered a couple stress fluid to study the impact of the squeeze film lubrication in circular stepped plates. In this investigation, the couple stress impact is governed by Stokes microcontinuum [11] theory and this study discovered the advantages of couple stress fluid compared to Newtonian lubricants, such as improved bearing's load capacity, reduced coefficient of friction and growth in squeeze film time.

However, it is well known that after having some run-in wear, bearing surfaces develop some roughness so, surface roughness and its impact on bearing performance have been deliberated by various investigators. Some mathematical models have been anticipated in the derivation of Reynolds type equations, which accounts for the surface roughness effect. Among all these models, the stochastic approach given by Christensen and Tonder [12–14] is used very widely. Many investigators have studied the combined influence of surface roughness and ferrofluid for a distinct porous bearing configuration [15–20]. All these scrutinies discovered that the load capacity of the bearing is improved due to ferrofluid and negatively skewed roughness. Andharia and Deheri [21] studied the effect of ferrofluid for longitudinally rough elliptical plates. Patel and Deheri [22] analysed the combined influence of ferrofluid and slip velocity for longitudinally rough conical plates and found that load capacity gets enhanced due to the magnetization and standard deviation. Shah and Patel [23] studied the influence of ferrofluid for a rotating sphere with a radially rough lower flat plate and shown that the overall performance of the sphere plate is improved due to a variable magnetic field. Lin [24] studied the influence of a magnetic fluid on journal bearings with longitudinal surface roughness and shown that the effects of longitudinal roughness suggest a growth in the load capacity along with a reduction in the friction parameter and the attitude angle compared to non-magnetic smooth surface case. The joint impact of surface roughness and couple stress on different bearing geometry is investigated by [25–27] and their investigations confirmed that the load capacity and squeeze film time increase due to the non-Newtonian behaviour of fluid compared to Newtonian case.

So, it is supposed to examine the influence of ferrofluid and longitudinal surface roughness on porous circular stepped plates in the presence of couple stress.

2. Analysis

Figure 1 displays the bearing geometry. The lower plate has porous facing, which remains fixed while the upper plate is moving with a squeeze velocity V. The fluid region is filled with incompressible ferrofluid with a couple stress effect. To characterize the surface roughness, the film thickness is taken as

$$H_i = h_i + h_s \quad \text{for} \quad i = 1, 2$$

where, h_i represents the mean film thickness and h_s is the quantity due to surface roughness calculated from mean level and is considered as a randomly changing quantity of non-zero mean. Additionaly, h_s is considered to be stochastic in nature having a polynomial form of a probability distribution function given by Christensen and Tonder [12–14]. The roughness parameters are stated by the relations

$$\alpha = E(h_s)$$
$$\sigma^2 = E\left[(h_s - \alpha)^2\right]$$
$$\varepsilon = E\left[(h_s - \alpha)^3\right]$$

Where the expectancy operator $E(\bullet)$ is described as

$$E(\bullet) = \int_{-\infty}^{\infty} (\bullet) f(h_s) dh_s$$

Through the traditional assumptions of hydrodynamic lubrication, the governing Reynolds type equation for the film pressure turns out be [10]

$$\frac{dp_i}{dr} = \frac{-6\mu V r}{S_i(H_i, l)} \tag{1}$$

$$S_i(h_i, l) = H_i^3 + 12\phi H - 12l^2 H_i + 24l^3 \tan h \left(\frac{H_i}{2l}\right) \tag{2}$$

for smooth bearing.

To derive the longitudinal surface roughness, we adopted the stochastic approach given by Christensen and Tonder [12–14] in equation (1).

$$\frac{dp_i}{dr} = \frac{-6\mu V r}{g_i(h_i, \alpha, \sigma, \varepsilon, l)} \tag{3}$$

where,

$$g_i(h_i, \alpha, \sigma, \varepsilon, l) = \frac{1}{E\left(H_i^{-3}\right)} + 12\phi H - 12l^2 \frac{1}{E\left(H_i^{-1}\right)} + 24l^3 \tan h \left(\frac{\frac{1}{E\left(H_i^{-1}\right)}}{2l}\right) \tag{4}$$

where,

$$g_i(h_i, \alpha, \sigma, \varepsilon, l) = \frac{1}{m_i(h_i, \alpha, \sigma, \varepsilon)} + 12\phi H - 12l^2 \frac{1}{n_i(h_i, \alpha, \sigma, \varepsilon)} + 24l^3 \tan h \left(\frac{\frac{1}{n_i(h_i, \alpha, \sigma, \varepsilon)}}{2l}\right) \tag{5}$$

$$m_i(h_i, \alpha, \sigma, \varepsilon) = h_i^{-3}\left(1 - 3\alpha h_i^{-1} + 6h_i^{-2}\left(\sigma^2 + \alpha^2\right) - 10h_i^{-3}\left(3\sigma^2\alpha + \alpha^3 + \varepsilon\right)\right) \tag{6}$$

$$n_i(h_i, \alpha, \sigma, \varepsilon) = h_i^{-1}\left(1 - \alpha h_i^{-1} + h_i^{-2}\left(\sigma^2 + \alpha^2\right) - h_i^{-3}\left(3\sigma^2\alpha + \alpha^3 + \varepsilon\right)\right) \tag{7}$$

Neuringer-Rosenswein [28] intended a simple model to define the stable flow of ferrofluids in the existence of

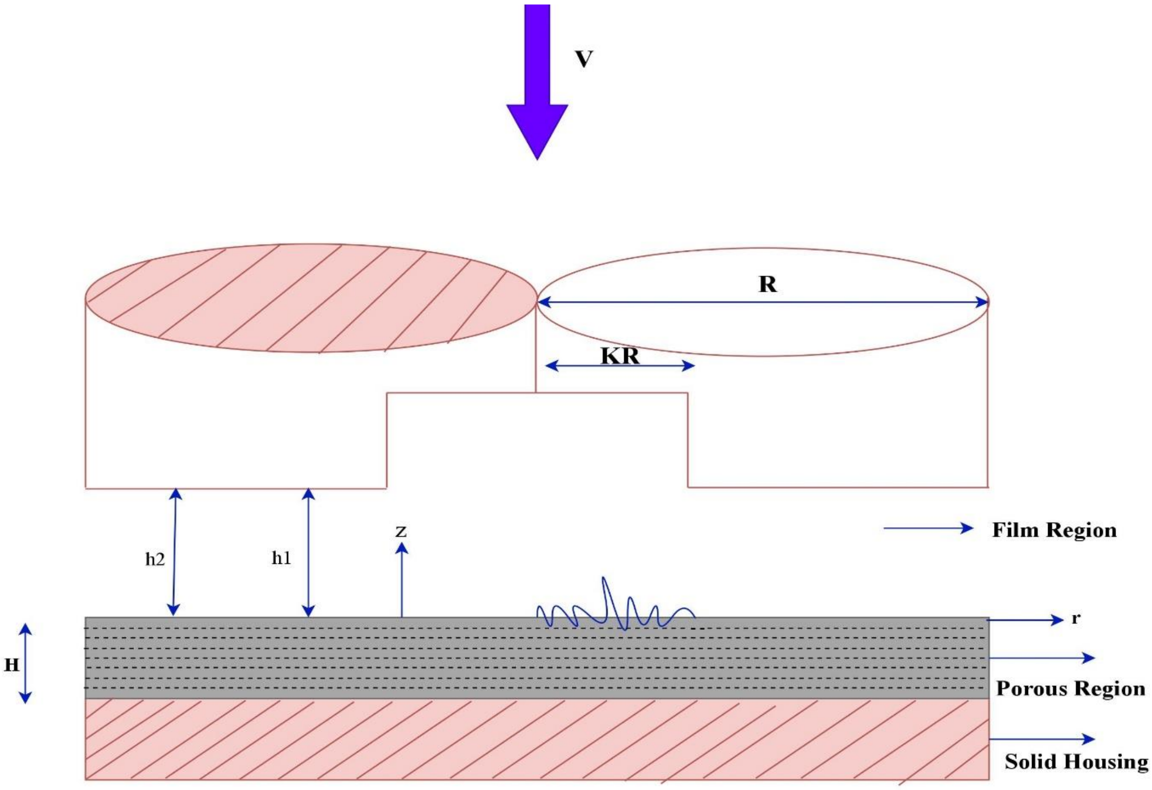

Figure 1. Physical configuration of circular step plates.

gradually varying magnetic fields. The model involves the following equations

$$\rho(\overline{q}\cdot\nabla)\overline{q} = -\nabla p + \mu\nabla^2\overline{q} + \mu_0(\overline{M}\cdot\nabla)\overline{H} \quad (8)$$

$$\nabla\cdot\overline{q} = 0 \quad (9)$$

$$\nabla\times\overline{H} = 0 \quad (10)$$

$$\overline{M} = \overline{\mu}\overline{H} \quad (11)$$

$$\nabla\cdot(\overline{H}+\overline{M}) = 0 \quad (12)$$

By using equation (10) and (11) in equation (8), it reduces to

$$\rho(\overline{q}\cdot\nabla)\overline{q} = -\nabla\left(p - \frac{\mu_0\overline{\mu}}{2}H^2\right) + \mu\nabla^2\overline{q} \quad (13)$$

Equation (13) represents that additional pressure term $\frac{1}{2}\mu_0\overline{\mu}H^2$ is present in the equation of motion when ferrofluid is used as a lubricant.

Therefore, in the context of Neuringer - Rosensweig [28] model, equation (3) transfer to

$$\frac{d}{dr}\left[p_i - 0.5\mu_0\overline{\mu}H^2\right] = \frac{-6\mu V r}{g_i(h_i,\alpha,\sigma,\varepsilon,l)} \quad (14)$$

in equation (14), H^2 denotes the magnetic field's magnitude and is given by

$$H^2 = A(R-r)(r-KR) \quad (15)$$

where A is an appropriate constant reliant on the material to yield a field of expected magnetic field strength. Where,

- $h_i = h_1$ minimum film thickness in the film region $0 \le r \le KR$ and
- $h_i = h_2$ maximum film thickness in the film region $KR \le r \le R$.

The related fluid film pressure boundary conditions are

$$p_1 = p_2 \text{ at } r = KR \quad \text{and} \quad p_2 = 0 \text{ at } r = R \quad (16)$$

The integration of equation (14) with respect to r with the boundary conditions given in expression (16) yields the pressure in both the film regions

$$p_1 = \frac{3\mu V}{g_1}(K^2R^2 - r^2) + \frac{3\mu V}{g_2}(R^2 - R^2K^2) + \\ + 0.5\mu_0\overline{\mu}H^2 \quad (17)$$

$$p_2 = \frac{3\mu V}{g_2}(R^2 - r^2) + 0.5\mu_0\overline{\mu}H^2 \quad (18)$$

where,

$$g_1 = \frac{1}{m_1(h_1,\alpha,\sigma,\varepsilon)} + 12\phi H - 12l^2\frac{1}{n_1(h_1,\alpha,\sigma,\varepsilon)} + \\ + 24l^3\tan h\left(\frac{\frac{1}{n_1(h_1,\alpha,\sigma,\varepsilon)}}{2l}\right) \quad (19)$$

$$g_2 = \frac{1}{m_2(h_2,\alpha,\sigma,\varepsilon)} + 12\phi H - 12l^2 \frac{1}{n_2(h_2,\alpha,\sigma,\varepsilon)} + \\ + 24l^3 \tan h \left(\frac{\frac{1}{n_2(h_2,\alpha,\sigma,\varepsilon)}}{2l} \right) \quad (20)$$

Integrating the expression (17) and (18), the load bearing capacity w is obtained as

$$w = 2\pi \int_0^{KR} p_1 r dr + 2\pi \int_{KR}^{R} p_2 r dr \quad (21)$$

which yields

$$w = \frac{\pi R^4 0.5 A\mu_0\overline{\mu}}{6}(1-2K) + \\ + \frac{3\pi\mu V R^4}{2}\left[\frac{K^4}{g_1} + \frac{(1-K^4)}{g_2}\right] \quad (22)$$

By making the use of following dimensionless variables in equation (22).

$$\mu^* = -\frac{\mu_0\overline{\mu}Ah_2^3}{\mu V}, H^* = \frac{h_1}{h_2}, l^* = \frac{2l}{h_2}, \alpha^* \frac{\alpha}{h_2}, \\ \sigma^* = \frac{\sigma}{h_2}, \varepsilon^* = \frac{\varepsilon}{h_2^3}, \psi = \frac{\phi H}{h_2^3} \quad (23)$$

Expression (22) transfers to dimensionless load capacity as follows.

$$\overline{w} = \frac{2wh_2^3}{3\pi\mu V R^4} = \frac{\mu^*(2K-1)}{18} + \left[\frac{K^4}{G_1} + \frac{(1-K^4)}{G_2}\right] \quad (24)$$

where,

$$G_1 = \frac{h_2^3}{g_1} = \frac{1}{M_1(H^*,\alpha^*,\sigma^*,\varepsilon^*)} + 12\psi - \\ - \frac{3l^{*2}}{N_1(H^*,\alpha^*,\sigma^*,\varepsilon^*)} + \\ + 3l^{*3} \tan h \left(\frac{1}{N_1(H^*,\alpha^*,\sigma^*,\varepsilon^*)l^*} \right) \quad (25)$$

$$G_2 = \frac{h_2^3}{g_2} = \frac{1}{M_2(\alpha^*,\sigma^*,\varepsilon^*)} + 12\psi - \\ - \frac{3l^{*2}}{N_2(\alpha^*,\sigma^*,\varepsilon^*)} + \\ + 3l^{*3} \tan h \left(\frac{1}{N_2(\alpha^*,\sigma^*,\varepsilon^*)l^*} \right) \quad (26)$$

where,

$$M_1(H^*,\alpha^*,\sigma^*,\varepsilon^*) = H^{*-3}(1 - 3\alpha^* H^{*-1} + \\ + 6H^{*-2}(\sigma^{*2} + \alpha^{*2}) - \\ - 10H^{*-3}(3\sigma^{*2}\alpha^* + \alpha^*3 + \varepsilon^*)) \quad (27)$$

$$N_1(H^*,\alpha^*,\sigma^*,\varepsilon^*) = H^{*-1}(1 - \alpha^* H^{*-1} + \\ + H^{*-2}(\sigma^{*2} + \alpha^{*2}) - \\ - H^{*-3}(3\sigma^{*2}\alpha^* + \alpha^*3 + \varepsilon^*)) \quad (28)$$

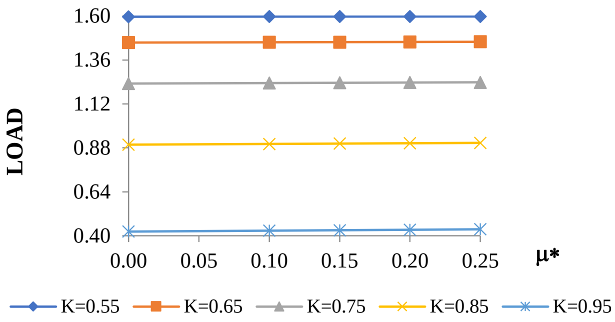

Figure 2. Profile of $\overline{w}$ for the combination of μ^* with various values K, with $H^* = 2.10$, $\sigma^* = 0.05$, $\alpha^* = -0.025$, $\varepsilon^* = -0.025$, $\psi = 0.001$ and $l^* = 0.3$.

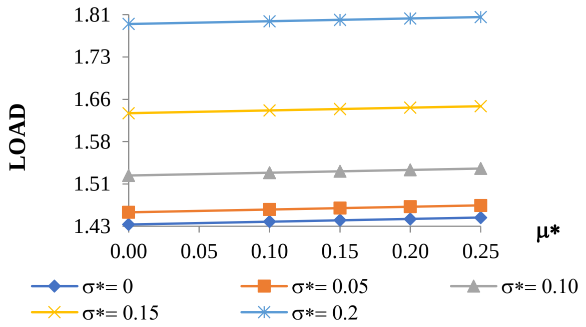

Figure 3. Profile of $\overline{w}$ for the combination of μ^* with various values σ^*, with $H^* = 2.10$, $K = 0.65$, $\alpha^* = -0.025$, $\varepsilon^* = -0.025$, $\psi = 0.001$ and $l^* = 0.3$.

$$M_2(\alpha^*,\sigma^*,\varepsilon^*) = (1 - 3\alpha^* + 6(\sigma^{*2} + \alpha^{*2}) - \\ - 10(3\sigma^{*2}\alpha^* + \alpha^*3 + \varepsilon^*)) \quad (29)$$

$$N_2(\alpha^*,\sigma^*,\varepsilon^*) = (1 - \alpha^* + (\sigma^{*2} + \alpha^{*2}) - \\ - (3\sigma^{*2}\alpha^* + \alpha^*3 + \varepsilon^*)) \quad (30)$$

3. Results and discussion

This study examined the performance characteristic of longitudinally rough porous circular stepped plates with ferrofluid in the presence of couple stress effect. The equation (17), equation (18) and equation (24) represent the closed form solution for pressure and load capacity. Equation (24) suggests that load capacity is enhanced by $\frac{\mu^*(2K-1)}{18}$ times as compared to a conventional lubricant based bearing system. Also, the comparison is made between the current results with the results obtained by [10], The effect of longitudinal surface roughness is described by the parameter $\sigma^*, \alpha^*, \varepsilon^*$. The variation of $\overline{w}$ with regards to μ^* for distinct values of $K, \sigma^*, \alpha^*, \varepsilon^*, \psi, l^*$ is displayed in Figures 2-7. One can notice from all these Figures that the effect of μ^* is an improvement of the load bearing capacity. From the physical perspective, μ^* increases the viscosity of the lubricant, which results in improved pressure and load capacity. Fig. 7 shows that the influence of μ^* is more emphasized for a larger value of l^*.

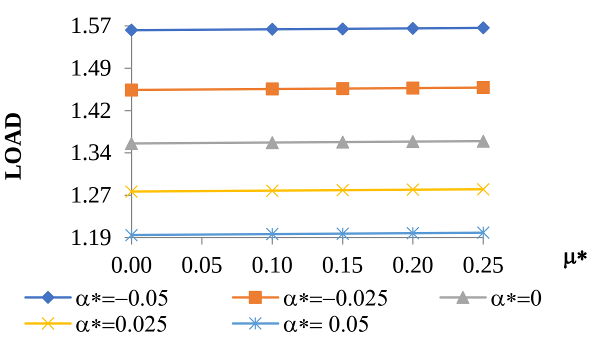

FIGURE 4. Profile of $\overline{w}$ for the combination of μ^* with various values α^*, with $H^* = 2.10$, $K = 0.65$, $\sigma^* = 0.05$, $\varepsilon^* = -0.025$, $\psi = 0.001$ and $l^* = 0.3$.

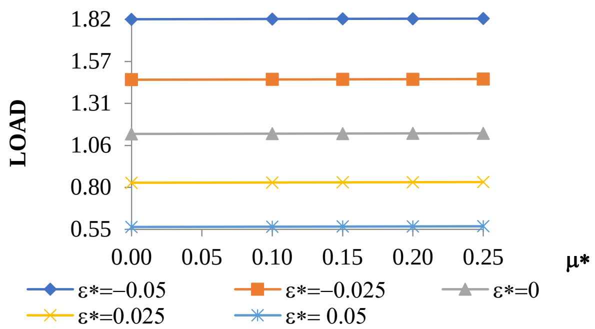

FIGURE 5. Profile of $\overline{w}$ for the combination of μ^* with various values ε^*, with $H^* = 2.10$, $K = 0.65$, $\sigma^* = 0.05$, $\alpha^* = -0.025$, $\psi = 0.001$ and $l^* = 0.3$.

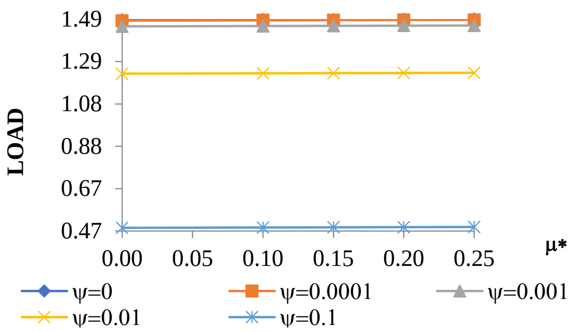

FIGURE 6. Change in $\overline{w}$ plotted for μ^* with various values of ψ, with $H^* = 2.10$, $K = 0.65$, $\sigma^* = 0.05$, $\alpha^* = -0.025$, $\varepsilon^* = -0.025$ and $l^* = 0.3$.

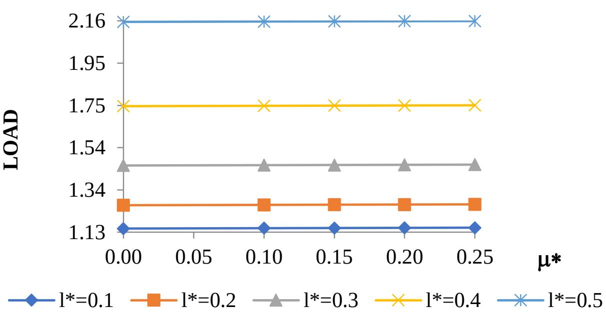

FIGURE 7. Variation of $\overline{w}$ plotted for μ^* with various values of l^*, with $H^* = 2.10$, $K = 0.65$, $\sigma^* = 0.05$, $\alpha^* = -0.025$, $\varepsilon^* = -0.025$ and $\psi = 0.001$.

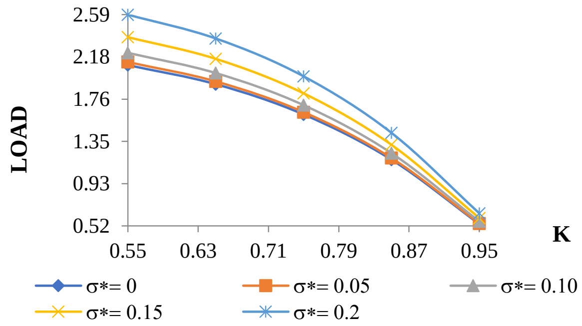

FIGURE 8. Profile of $\overline{w}$ referenced to K for various values of σ^*, with $H^* = 2.10$, $\mu^* = 0.15$, $\alpha^* = -0.025$, $\varepsilon^* = -0.025$, $\psi = 0.001$ and $l^* = 0.3$.

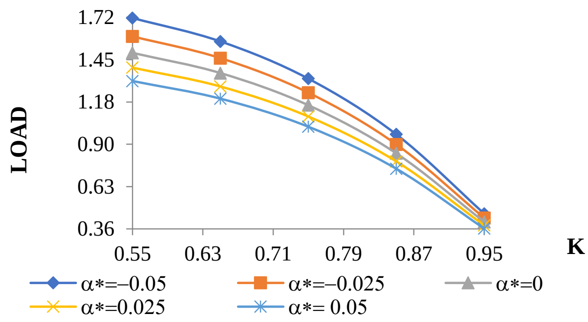

FIGURE 9. Trends of $\overline{w}$ referenced to K for various values of α^*, with $H^* = 2.10$, $\mu^* = 0.15$, $\sigma^* = 0.05$, $\varepsilon^* = -0.025$, $\psi = 0.001$ and $l^* = 0.3$.

Figures 8 - 12 represent the influence of K on $\overline{w}$ for various values of $\sigma^*, \alpha^*, \varepsilon^*, \psi$ and l^*. From all these Figures, one can conclude that $\overline{w}$ decreases as the value of K increases. Also, Figure 12 suggests that the decrease of $\overline{w}$ is insignificant for higher values of l^*.

Distribution of $\overline{w}$ with regard to H^* for distinct values of $\sigma^*, \alpha^*, \varepsilon^*, \psi$ and l^* is presented in Figures 13 - 17. It can be seen that $\overline{w}$ decreases as the value of H^* increases and that the decrease of $\overline{w}$ is minimal when H^* surpasses the value of 2.26.

Figures 18 - 21 characterize the positive impact of σ^* on the load capacity for various values of $\alpha^*, \varepsilon^*, \psi, l^*$. All these Figures show that there is a sharp growth in $\overline{w}$ as the values of σ^* increase. In the case of longitudinal surface roughness, the parameter σ^* plays a crucial role as it supports the motion of the lubricant, which results in an increased pressure, and therefore load capacity. Figure 21 suggests that the maximum load is registered when $l^* = 0.5$ and $\sigma = 0.2$.

The positive influence of ε^* on $\overline{w}$ with regards to ψ and l^* can be seen from Figures 22 - 23. From both these Figures, one can observe that a negative increase in the values of ε^* rises the dimensionless load capacity of bearing. So, the optimistic impact of ε^* may be accordingly considered while designing the bearing structure. Figures 6, 11, 16, 20 and 22 clearly show that the initial impact of porous facing is insignificant up to a value of $\psi = 0.001$.

K	l^*	$\overline{w}$ for the present study with $\begin{pmatrix} \mu^* = 0.15, & \sigma^* = 0.15, \\ \alpha^* = -0.025, & \varepsilon = -0.025, \\ \psi = 0.001, & H^* = 2.10 \end{pmatrix}$	$\overline{w}$ obtained from [10]	Relative percentage growth in $\overline{w}$ ($R_{\overline{w}}$)
	0.1	1.2578614535	0.9436490018	33.30
0.55	0.3	1.5970615126	1.1309267877	41.22
	0.5	2.3701103455	1.4970075375	58.32
	0.1	0.9786901999	0.7369511955	32.80
0.75	0.3	1.2353809760	0.8791740326	40.52
	0.5	1.8198623988	1.1571299684	57.27
	0.1	0.3563430762	0.2791647245	27.65
0.95	0.3	0.4302954180	0.3216015680	33.80
	0.5	0.5971448849	0.4043820041	47.67

Table 1. Change in $\overline{w}$ and $R_{\overline{w}}$ for distinct values of K and l^*.

H	l^*	$\overline{w}$ for the present study with $\begin{pmatrix} \mu^* = 0.15, & \sigma^* = 0.15, \\ \alpha^* = -0.025, & \varepsilon = -0.025, \\ \psi = 0.001, & K = 0.65 \end{pmatrix}$	$\overline{w}$ obtained from [10]	Relative percentage growth in $\overline{w}$ ($R_{\overline{w}}$)
	0.1	1.23184347	0.92689311	32.90
1.3	0.3	1.55161185	1.10583213	40.31
	0.5	2.27664670	1.45544961	56.42
	0.1	1.15524444	0.86369031	33.76
2.1	0.3	1.46252673	1.03353911	41.51
	0.5	2.16263041	1.36552978	58.37
	0.1	1.14218948	0.85163399	34.12
2.9	0.3	1.44862282	1.02073256	41.92
	0.5	2.14709608	1.35128724	58.89

Table 2. Change in $\overline{w}$ and $R_{\overline{w}}$ for distinct values of H^* and l^*.

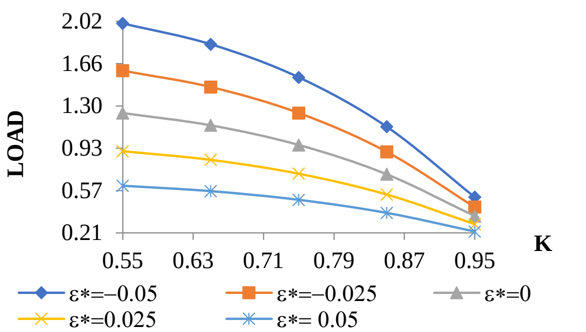

Figure 10. Trends of $\overline{w}$ referenced to K for various values of ε^*, with $H^* = 2.10$, $\mu^* = 0.15$, $\sigma^* = 0.05$, $\alpha^* = -0.025$, $\psi = 0.001$ and $l^* = 0.3$.

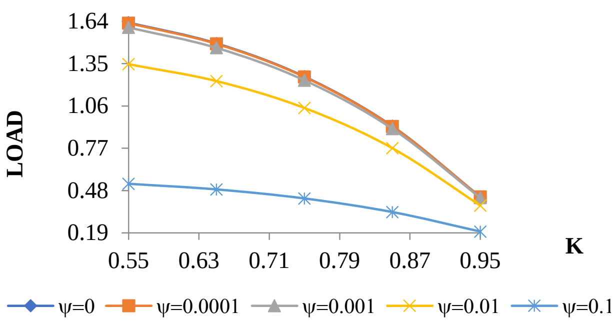

Figure 11. Trends of $\overline{w}$ referenced to K for various values of ψ^*, with $H^* = 2.10$, $\mu^* = 0.15$, $\sigma^* = 0.05$, $\varepsilon^* = -0.025$, $\alpha^* = -0.025$ and $l^* = 0.3$.

Tables 1 - 2 clearly show that the bearing's performance improves due to the combined influence of ferrofluid and couple stress when compared to the results obtained from [10]. It can be seen from Table 1 that there is a growth of about 58 % in $\overline{w}$ when $K = 0.55$ and $l^* = 0.5$. Also, from Table 2, it can be seen that a relative increase in $\overline{w}$ is around 59 % when $H^* = 2.9$ and $l^* = 0.5$.

4. Conclusion

The combined impact of surface roughness and ferrofluid for porous circular stepped plates in the presence of couple stress is analysed. The graphical and tabular results show that the combined impact of ferrofluid and couple stress improves the load bearing capacity considerably. Furthermore, this improvement in load bearing capacity is almost 58 % higher when

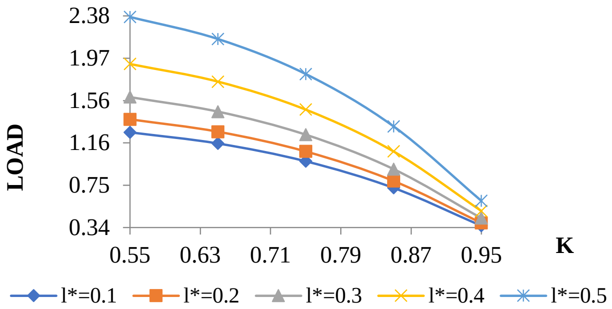

Figure 12. Trends of $\overline{w}$ referenced to K for various values of l^*, with $H^* = 2.10$, $\mu^* = 0.15$, $\sigma^* = 0.05$, $\varepsilon^* = -0.025$, $\alpha^* = -0.025$ and $\psi = 0.001$.

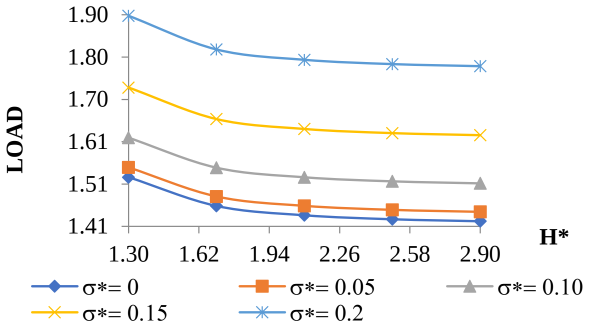

Figure 13. Trends of $\overline{w}$ referenced to H^* for various values of σ^*, with $K = 0.65$, $\psi = 0.001$, $\mu^* = 0.15$, $\varepsilon^* = -0.025$, $\alpha^* = -0.025$ and $l^* = 0.3$.

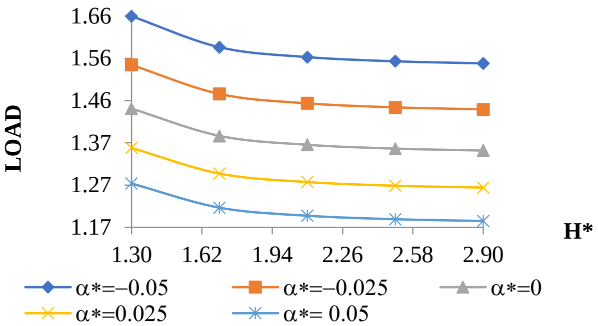

Figure 14. Trends of $\overline{w}$ referenced to H^* for various values of α^*, with $K = 0.65$, $\psi = 0.001$, $\mu^* = 0.15$, $\varepsilon^* = -0.025$, $\sigma^* = 0.05$ and $l^* = 0.3$.

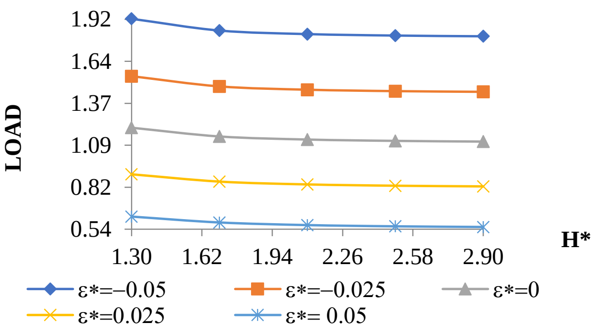

Figure 15. Trends of $\overline{w}$ referenced to H^* for various values of ε^*, with $K = 0.65$, $\psi = 0.001$, $\mu^* = 0.15$, $\alpha^* = -0.025$, $\sigma^* = 0.05$ and $l^* = 0.3$.

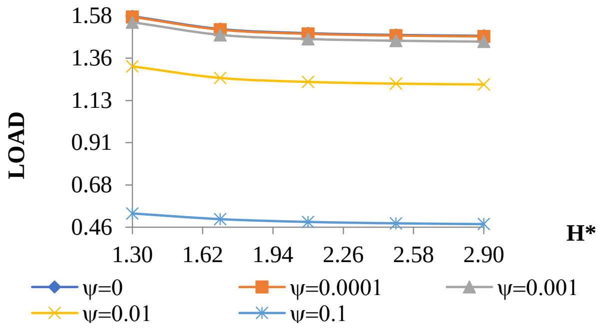

Figure 16. Trends of $\overline{w}$ referenced to H^* for various values of ψ, with $K = 0.65$, $\alpha^* = -0.025$, $\mu^* = 0.15$, $\varepsilon^* = -0.025$, $\sigma^* = 0.05$ and $l^* = 0.3$.

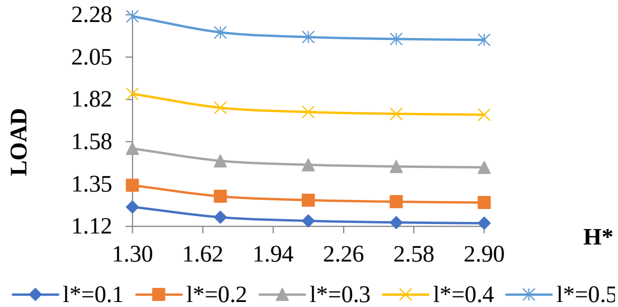

Figure 17. Trends of $\overline{w}$ referenced to H^* for various values of l^*, with $K = 0.65$, $\alpha^* = -0.025$, $\mu^* = 0.15$, $\varepsilon^* = -0.025$, $\sigma^* = 0.05$ and $\psi = 0.001$.

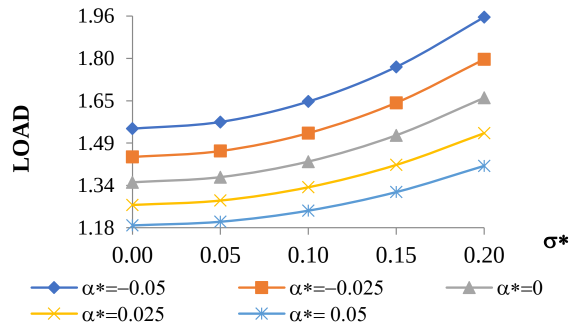

Figure 18. Distribution of $\overline{w}$ referenced to σ^* for various values of α^*, with $K = 0.65$, $\psi = 0.001$, $\mu^* = 0.15$, $\varepsilon^* = -0.025$, $H^* = 2.10$ and $l^* = 0.3$.

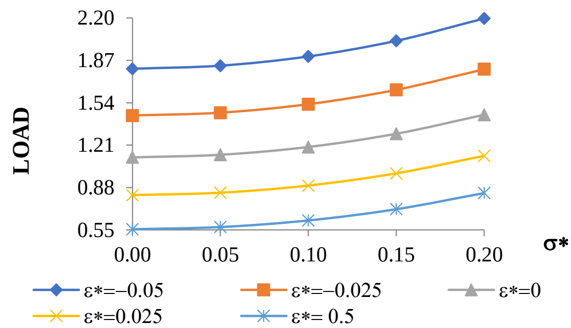

Figure 19. Distribution of $\overline{w}$ referenced to σ^* for various values of ε^*, with $K = 0.65$, $\psi = 0.001$, $\mu^* = 0.15$, $\alpha^* = -0.025$, $H^* = 2.10$ and $l^* = 0.3$.

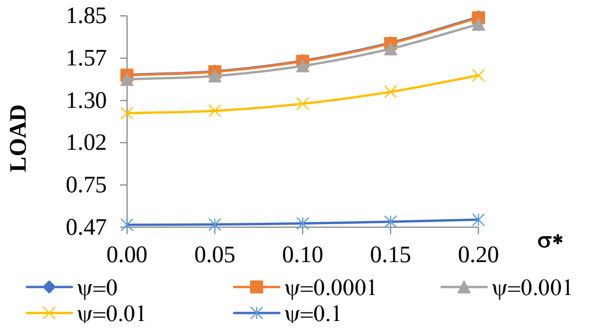

Figure 20. Distribution of $\overline{w}$ referenced to σ^* for various values of ψ, with $K = 0.65$, $\alpha^* = -0.025$, $\mu^* = 0.15$, $\varepsilon^* = -0.025$, $H^* = 2.10$ and $l^* = 0.3$.

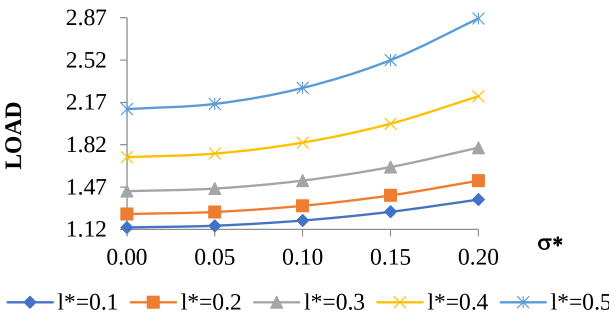

Figure 21. Distribution of $\overline{w}$ referenced to σ^* for various values of l^*, with $K = 0.65$, $\alpha^* = -0.025$, $\mu^* = 0.15$, $\varepsilon^* = -0.025$, $H^* = 2.10$ and $\psi = 0.001$.

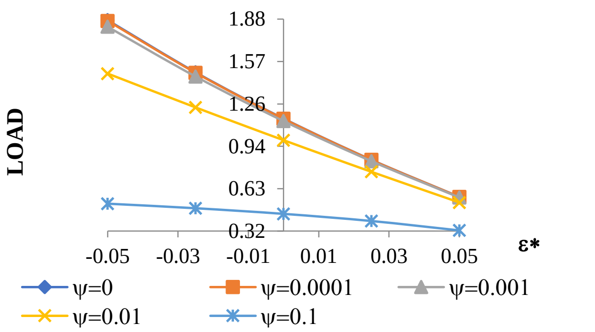

Figure 22. Distribution of $\overline{w}$ referenced to ε^* for various values of ψ, with $K = 0.65$, $\alpha^* = -0.025$, $\mu^* = 0.05$, $\sigma^* = 0.15$, $H^* = 2.10$ and $l^* = 0.3$.

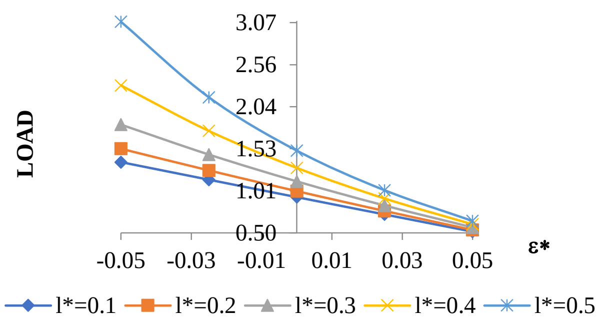

Figure 23. Distribution of $\overline{w}$ referenced to ε^* for various values of l^*, with $K = 0.65$, $\alpha^* = -0.025$, $\mu^* = 0.15$, $\sigma^* = 0.05$, $H^* = 2.10$ and $\psi = 0.001$.

compared to the results obtained from [10]. Also, the development in load capacity is enhanced in the presence of a standard deviation and negatively skewed roughness with a couple stress parameter. The reduction in load is due to the porous facing and positively skewed roughness can be compensated by employing the ferrofluid as a lubricant with the suitable choice of a couple stress parameter through which the life span of a circular step bearing can be boosted.

Acknowledgements

The authors acknowledge the valuable remarks and suggestions of the reviewers, which have contributed to the development of the presentation and organization of the manuscript.

List of symbols

H porous facing thickness [mm]
H^* dimensionless fluid film thickness
$\overline{H}$ magnetic field vector
h_1 maximum fluid film thickness [mm]
h_2 minimum fluid film thickness [mm]
KR step location $(0 < K < 1)$
l couple stress parameter $\left(\sqrt{\frac{\eta}{\mu}}\right)$
l^* dimensionless couple stress parameter
$\overline{M}$ magnetization vector
p_1 film pressure for the region $(0 < r < KR)$
p_2 film pressure for the region $(KR < r < R)$
$\overline{q}$ fluid velocity vector
r radial coordinate
R radius of the circular plate
V squeeze velocity
w load capacity of bearing [N]
$\overline{w}$ dimensionless load capacity
α variance [mm]
α^* dimensionless variance
ε skewness [mm^3]
ε^* dimensionless skewness
η couple stress constant of the lubricant
μ fluid viscosity [N S/m^2]
μ_0 permeability of the free space
$\overline{\mu}$ magnetic susceptibility of particle
μ^* dimensionless magnetization parameter
σ standard deviation [mm]
σ^* dimensionless standard deviation
ϕ porous facing permeability
ψ porosity of porous facing

References

[1] M. Bhat, G. Deheri. Magnetic-fluid-based squeeze film in curved porous circular discs. *Journal of Magnetism and Magnetic Materials* **127**(1):159 – 162, 1993. doi:10.1016/0304-8853(93)90210-S.

[2] R. Shah. Ferrofluid lubrication in step bearing with two steps. *Industrial Lubrication and Tribology* **55**(6):265 – 267, 2003. doi:10.1108/00368790310496392.

[3] D. Kumar, P. Sinha, P. Chandra. Ferrofluid squeeze film for spherical and conical bearings. *International Journal of Engineering Science* **30**(5):645 – 656, 1992. DOI:10.1016/0020-7225(92)90008-5.

[4] R. Shah, M. Bhat. Ferrofluid squeeze film between curved annular plates including rotation of magnetic particles. *Journal of Engineering Mathematics* **51**:317 – 324, 2005. DOI:10.1007/s10665-004-1770-9.

[5] V. K. Agrawal. Magnetic-fluid-based porous inclined slider bearing. *Wear* **107**(2):133 – 139, 1986. DOI:10.1016/0043-1648(86)90023-2.

[6] G. Ramanaiah, P. Sarkar. Squeeze films and thrust bearings lubricated by fluids with couple stress. *Wear* **48**(2):309 – 316, 1978. DOI:10.1016/0043-1648(78)90229-6.

[7] J.-R. Lin. Squeeze film characteristics of finite journal bearings: couple stress fluid model. *Tribology International* **31**(4):201 – 207, 1998. DOI:10.1016/S0301-679X(98)00022-X.

[8] G. Maiti. Composite and step slider bearings in micropolar fluid. *Japanese Journal of Applied Physics* **12**(7):1058 – 1064, 1973. DOI:10.1143/jjap.12.1058.

[9] J.-R. Lin, C.-R. Hung, R.-F. Lu. Averaged inertia principle for non-Newtonian squeeze films in wide parallel plates: Couple stress fluid. *Journal of Marine Science and Technology* **14**:218 – 224, 2006.

[10] N. B. Naduvinamani, A. Siddangouda. Squeeze film lubrication between circular stepped plates of couple stress fluids. *Journal of The Brazilian Society of Mechanical Sciences and Engineering* **31**(1):21 – 26, 2009. DOI:10.1590/S1678-58782009000100004.

[11] V. K. Stokes. *Theories of Fluids with Microstructure*, chap. Couple Stresses in Fluids. Springer, Berlin, 1984. DOI:10.1007/978-3-642-82351-0_4.

[12] H. Christensen, K. Tonder. Tribology of rough surface: Stochastic models of hydrodynamic lubrication. Sintef report 10/69, SINTEF, 1969a.

[13] H. Christensen, K. Tonder. Tribology of rough surfaces: parametric study and comparison of lubrication model. Sintef report 22/69, SINTEF, 1969b.

[14] H. Christensen, K. Tonder. The hydrodynamic lubrication of rough bearing surfaces of finite width. In *ASME-ASLE Lubrication Conference*, pp. 12 – 15. 1970.

[15] M. Shimpi, G. M. Deheri. Magnetic fluid-based squeeze film performance in rotating curved porous circular plates: The effect of deformation and surface roughness. *Tribology in Industry* **34**(2):57 – 67, 2012.

[16] R. M. Patel, G. M. Deheri, H. C. Patel. Effect of surface roughness on the behavior of a magnetic fluid-based squeeze film between circular plates with porous matrix of variable thickness. *Acta Polytechnica Hungarica* **8**(5):171 – 191, 2011.

[17] S. Snehal, G. Deheri. Effect of slip velocity on magnetic fluid lubrication of rough porous rayleigh step bearing. *Journal of Mechanical Engineering and Sciences* **4**:532 – 547, 2013. DOI:10.15282/jmes.4.2013.17.0050.

[18] Y. Vashi, R. Patel, G. M. Deheri. Ferrofluid based squeeze film lubrication between rough stepped plates with couple stress effect. *Journal of Applied Fluid Mechanics* **11**(3):597 – 612, 2018. DOI:10.29252/jafm.11.03.27854.

[19] M. Munshi, A. Patel, G. Deheri. A study of ferrofluid lubrication based rough sine film slider bearing with assorted porous structure. *Acta Polytechnica* **59**(2):144 – 152, 2019. DOI:10.14311/AP.2019.59.0144.

[20] S. R. Mishra, M. Barik, G. Dash. An analysis of hydrodynamic ferrofluid lubrication of an inclined rough slider bearing. *Tribology - Materials, Surfaces & Interfaces* **12**(1):1 – 10, 2018. DOI:10.1080/17515831.2017.1418280.

[21] P. Andharia, G. M. Deheri. Performance of magnetic-fluid-based squeeze film between longitudinally rough elliptical plates. *ISRN Tribology* **2013**, 2013. DOI:10.5402/2013/482604.

[22] J. Patel, G. M. Deheri. The effect of slip velocity on the ferrofluid based squeeze film in longitudinally rough conical plates. *Journal of Serbian Society for Computational Mechanics* **10**(2):18 – 29, 2016. DOI:10.5937/jsscm1602018P.

[23] R. Shah, D. Patel. On the ferrofluid lubricated squeeze film characteristics between a rotating sphere and a radially rough plate. *Meccanica* **51**:1973 – 1984, 2016. DOI:10.1007/s11012-015-0337-3.

[24] J.-R. Lin. Longitudinal surface roughness effects in magnetic fluid lubricated journal bearings. *Journal of Marine Science and Technology* **24**:711 – 716, 2016. DOI:10.6119/JMST-016-0201-1.

[25] N. Naduvinamani, A. Siddangouda. Effect of surface roughness on the hydrodynamic lubrication of porous step-slider bearings with couple stress fluids. *Tribology International* **40**(5):780 – 793, 2007. DOI:10.1016/j.triboint.2006.07.003.

[26] A.Siddangouda. Combined effects of surface roughness and non-newtonian couple stresses squeeze film characteristics between parallel stepped plates. *International Journal of Mathematical* **6**(2):113 – 121, 2015.

[27] N. B. Naduvinamani, K. Biradar. Surface roughness effects on curved pivoted slider bearings with couple stress fluid. *Lubrication Science* **18**:293 – 307, 2006. DOI:10.1002/ls.24.

[28] J. L. Neuringer, R. Rosensweig. Magnetic fluids. *Physics of fluids* **7**(12):1927 – 1937, 1964.